

The Life Cycle of a Tornadic Cloud as Seen from a Geosynchronous Satellite

R. J. Hung*

The University of Alabama, Huntsville, Alabama

James C. Dodge†

NASA Headquarters, Washington, D.C.

and

Robert E. Smith‡

NASA George C. Marshall Space Flight Center, Huntsville, Alabama

The life span of a severe storm is on the order of a few hours. Rapid-scan infrared and visible observations from geosynchronous satellites can be useful for studying the life cycle of a severe convective storm. By using artificial colors for pixels representing blackbody temperatures of the cloud top, convective storms can be observed throughout their life cycles. In this paper clouds associated with a tornadic storm, the Ringwood, Okla. tornado on May 29, 1977, are compared with those without a tornadic storm to illustrate how the infrared and visible observations from a geosynchronous satellite can be used to study the differences in their life cycles. The instability of the air mass and the meteorological background are discussed based on balloon observations.

Introduction

GEOSYNCHRONOUS satellite visible and infrared observations provide a powerful tool for studying severe convective storms, such as thunderstorms, tornadoes, hail storms, hurricanes, etc.¹⁻⁶ The infrared image provides an indication of the equivalent blackbody temperature of the observed cloud tops. In the Geosynchronous Operational Environmental Satellite (GOES) infrared sensor, 256 different digital count values are assigned to represent specific ranges of blackbody temperatures. By referencing the temperature/height and humidity profiles from conventional rawinsonde observations (the background meteorological data for the instability of the air mass) to the satellite infrared data sets at different time periods, the development of convective clouds can be studied in detail from the formation of the cloud and the initiation of the updraft motion to the development of the tornadic cloud.

In this article the life cycles of two isolated cloud systems in Oklahoma on May 28-29, 1977, are used to illustrate how the visible and infrared images observed from a geosynchronous satellite can be utilized to study severe storm development. A comparison of the life cycles of these isolated clouds systems, one of which eventually spawned a tornado at Ringwood, Okla., shows that it is very difficult to distinguish any significant differences during the infancy and developing stages of the cloud system. There are, however, some special features of the cloud associated with the tornado. These special features are the very low cloud top temperature of the overshooting turret, a much higher growth rate of the cloud top above the tropopause, and a much larger area above the tropopause.

Satellite Infrared Images

An image data processing system (IDAPS), developed by the NASA Marshall Space Flight Center for the image

processing requirements of the Skylab experiments, was used to process the high-resolution satellite photographs, both visible and infrared. An isolated cloud system in north central Oklahoma (at Ringwood) which spawned a tornado on May 28-29, 1977, is compared with an isolated thunderstorm system located in south central Oklahoma at about the same time.

Cumulative histograms are compiled starting from the cold end of the temperature distribution. The number of pixels N_i with blackbody temperature equal to or less than temperature T_i is obtained. Physically this number is roughly equal to the area of the cloud top with temperature $\leq T_i$. By referencing those data to a standard sounding, the horizontal area of the cloud penetrating above certain altitudes can be determined.

GOES digital infrared (IR) data for the entire United States during the period 2116 GMT, May 28, to 0203 GMT, May 29, 1977, were analyzed in this study. The period between observations was 15 min. In this time period, two isolated clouds systems were identified, one associated with a tornado (cloud A) located in north central Oklahoma and the other without a tornado (cloud B) located in south central Oklahoma.

Figures 1-9 are the pseudocolor representations of the cloud top temperatures in Oklahoma and portions of the surrounding states during the period 2116 GMT, May 28 to 0203 GMT, May 29, 1977. The color code for Figs. 1-9 is shown in Table 1.

From visible data, cloud A started to form at 2333 GMT while cloud B formed at 2201 GMT. The rawinsonde observation at Oklahoma City at 2300 GMT, May 28, 1977, showed that the tropopause temperature was -65°C ; therefore the white, red, and yellow false colors were for

Table 1 Color code for Figs. 1-9

| Color | Temperature range, $^\circ\text{C}$ |
|--------|-------------------------------------|
| Orange | ≥ -2.7 |
| Blue | -3.2 to -22.7 |
| Green | -23.7 to -54.2 |
| Purple | -55.2 to -66.2 |
| White | -67.2 to -69.2 |
| Red | -70.2 to -72.2 |
| Yellow | ≤ -73.2 |

Received April 26, 1982; revision received Oct. 21, 1982. This paper is declared a work of the U.S. Government and therefore is in the public domain.

*Professor, School of Science and Engineering. Associate Fellow AIAA.

†Manager, Severe Storms and Local Weather Research Program.

‡Deputy Chief, Division of Atmospheric Science.



Fig. 1 Pseudocolor representation of the cloud top temperatures in Oklahoma and surrounding states from GOES infrared image at 2116 GMT, May 28, 1977.



Fig. 2 Pseudocolor representation of the cloud top temperatures in Oklahoma and surrounding states from GOES infrared image at 2131 and 2201 GMT, May 28, 1977. Cloud B started to form in south central Oklahoma at 2201 GMT.

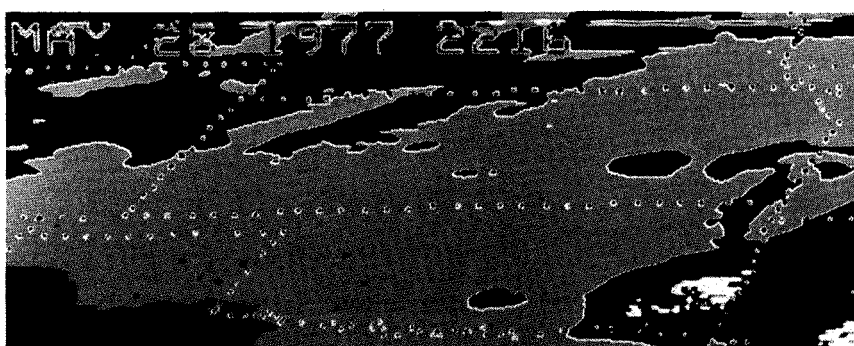


Fig. 3 Pseudocolor representation of the cloud top temperatures in Oklahoma and surrounding states from GOES infrared image at 2216 and 2231 GMT, May 28, 1977. The white spot of cloud B with cloud top height penetrating above tropopause started to appear at 2231 GMT.

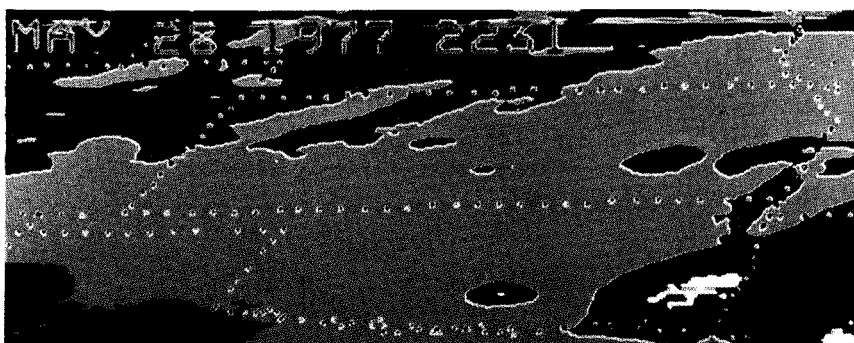


Fig. 4 Pseudocolor representation of the cloud top temperatures in Oklahoma and surrounding states from GOES infrared image at 2302 and 2333 GMT, May 28, 1977. Cloud A started to form in north central Oklahoma at 2333 GMT.

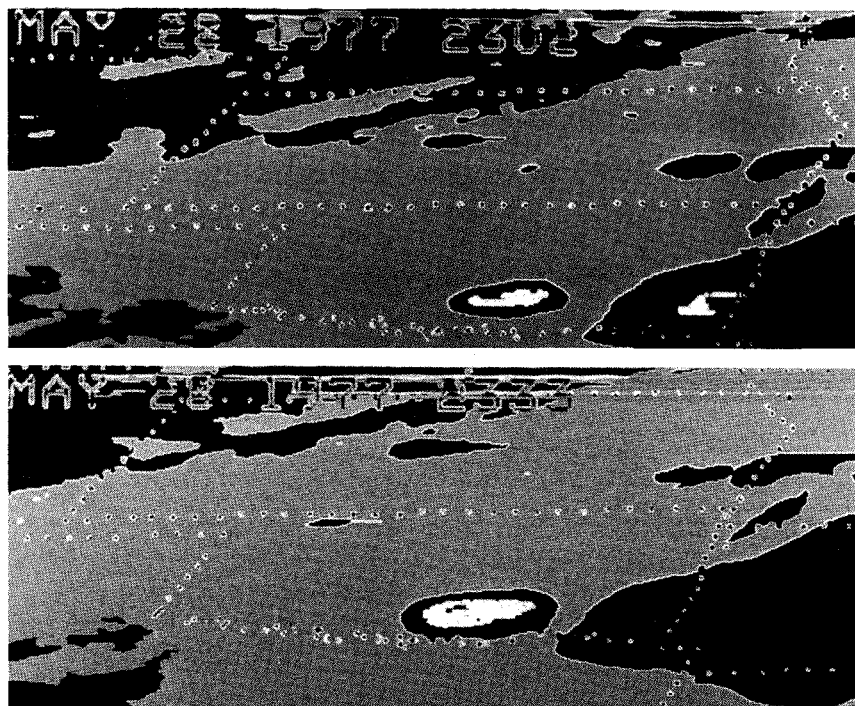
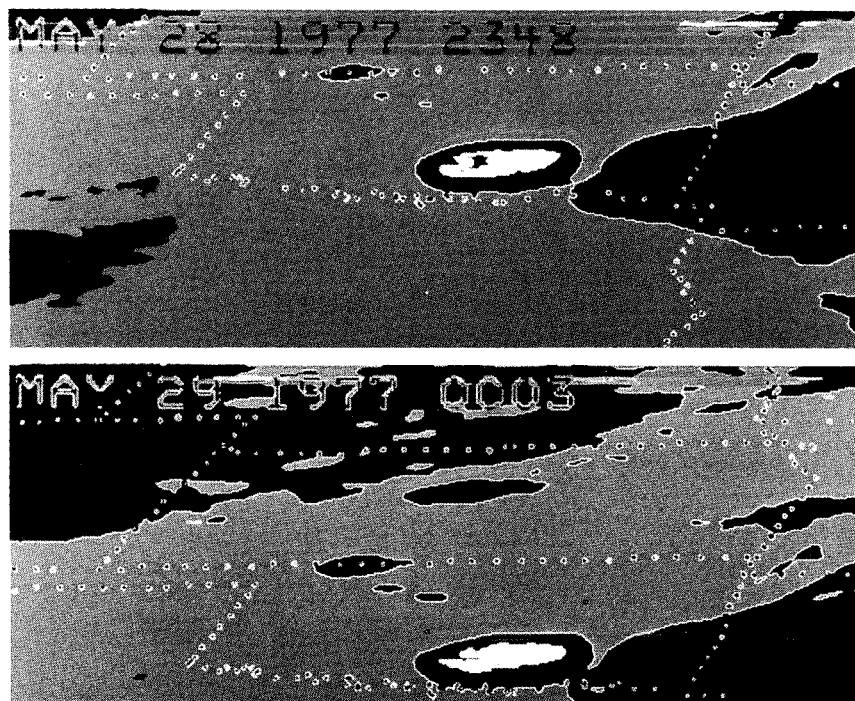


Fig. 5 Pseudocolor representation of the cloud top temperatures in Oklahoma and surrounding states from GOES infrared image at 2348 and 0003 GMT, May 28-29, 1977. Cloud system A started to penetrate above tropopause, with white spot in the figure, at 0003 GMT.



clouds above the tropopause. Based on radar summaries, the clouds located in southeastern Oklahoma were cirrus clouds without thunderstorm activity. In approximately half an hour after becoming identifiable on the visible images both cloud systems tops had reached the tropopause, system A at 2333-0003 GMT and system B at 2201-2231 GMT. In this respect, there was very little or no difference between the two systems.

After penetrating the tropopause, clouds A and B show somewhat different characteristics. About 1 h after penetrating the tropopause, 0101 GMT, the top of cloud system A reached a temperature in the range -70.2 to -72.2°C . The area of the cloud top with this temperature continued to expand until 0148 GMT as the cloud top grew

and expanded vertically until it reached a temperature $\leq -73.2^{\circ}\text{C}$. A tornado spawned by this system touched down at 0205 GMT. The infrared imagery of the bottom picture of Fig. 9 illustrates the cloud top temperature distribution of cloud system A, located at north central Oklahoma, 2 min prior to the touchdown of the tornado. On the other hand, the cloud top temperature change for system B was small and within a range of another 3°C decrease after the penetration of the tropopause. This cloud then started to dissipate at 0033 GMT, as shown in Fig. 6 for the cloud located at south central Oklahoma, about 2 h after the penetration of the tropopause. During this time, radar echoes showed enhanced thunderstorm activity at the location of cloud system B.

Figure 10 is a histogram of cloud A after it penetrated the tropopause. As the cloud grew, the top reached an equivalent blackbody temperature T_{BB} of $< -65.3^{\circ}\text{C}$ at 0003 GMT, $\leq -67.2^{\circ}\text{C}$ at 0033 GMT, $\leq -72.2^{\circ}\text{C}$ at 0103 GMT, and the lowest temperature $\leq -74.2^{\circ}\text{C}$ at 0148 GMT. The area of the cloud top with temperature $\leq -72.2^{\circ}\text{C}$ reached its maximum value at 0133 GMT, gradually decreased until 0148 GMT, and then sharply decreased. The tornado finally touched down at 0205 GMT, apparently as the cloud top was rapidly collapsing. This result is in good agreement with the aircraft observations made by Fujita and his associates.^{7,8} Based on *Storm Data*, issued by the National Climate Center, the tornado was on the ground 15 km south of Ringwood, Major County, Okla., at 0205 GMT.

Figure 11 is a similar histogram for cloud B. As the cloud grew, the top reached a temperature of -67.2°C at 2231 GMT, -68.2°C at 2333 GMT, and -68.2°C at 2333 GMT.

A comparison of the rawinsonde observation and the infrared observations from the satellite shows that the temperature for cloud A is 9°C colder than the tropopause and for cloud B 3°C colder. With these temperature differences the density of the overshooting turret is much higher than the density of the surrounding air; therefore, the overshooting turret can exist only as long as it is dynamically supported by intense vertical convection. Where the internal vertical convection can no longer support this excess mass, the overshooting turret collapses. A comparison of Figs. 10 and 11 shows that the maximum area of the overshooting turret

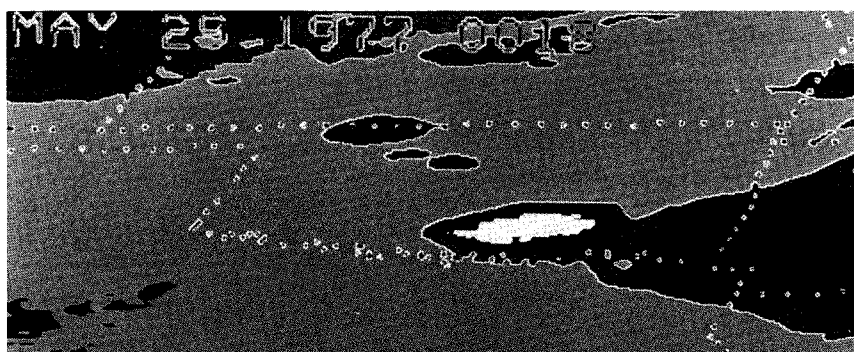


Fig. 6 Pseudocolor representation of the cloud top temperatures in Oklahoma and surrounding states from GOES infrared image at 0018 and 0033 GMT, May 29, 1977.

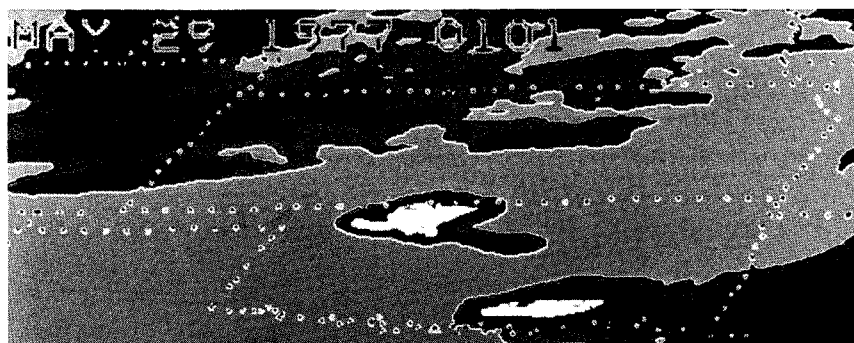
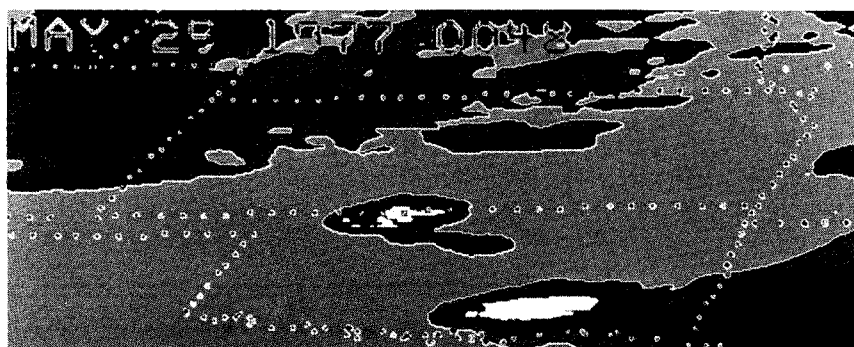


Fig. 7 Pseudocolor representation of the cloud top temperatures in Oklahoma and surrounding states from GOES infrared image at 0048 and 0101 GMT, May 29, 1977. The top of cloud system A reached a temperature in the range -70.2 to -72.2°C (red spot in the figure) at 0101 GMT.

Fig. 8 Pseudocolor representation of the cloud top temperatures in Oklahoma and surrounding states from GOES infrared image at 0118 and 0133 GMT, May 29, 1977. The red spot of cloud system A continued to expand during this period.

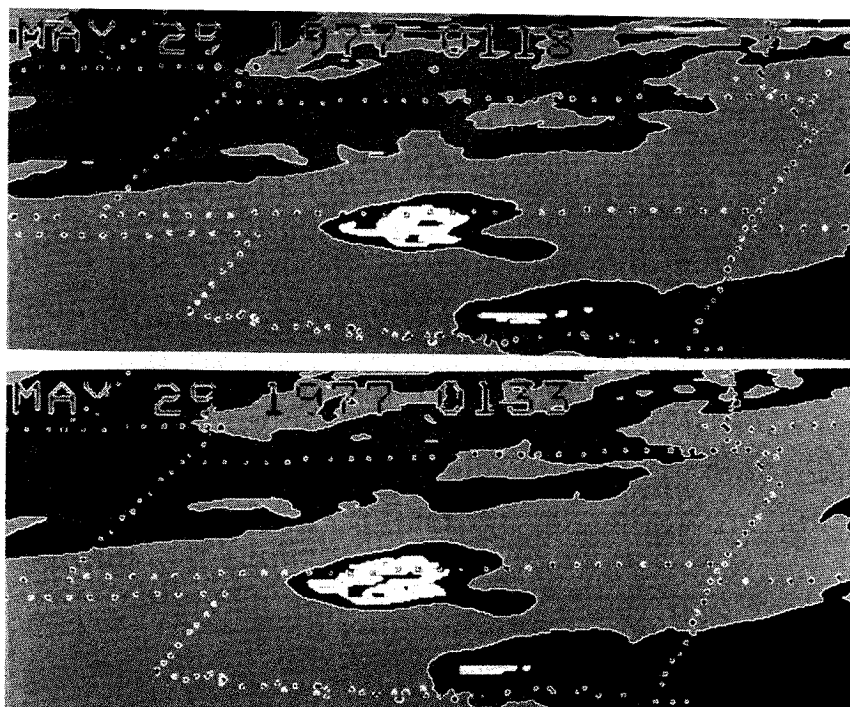
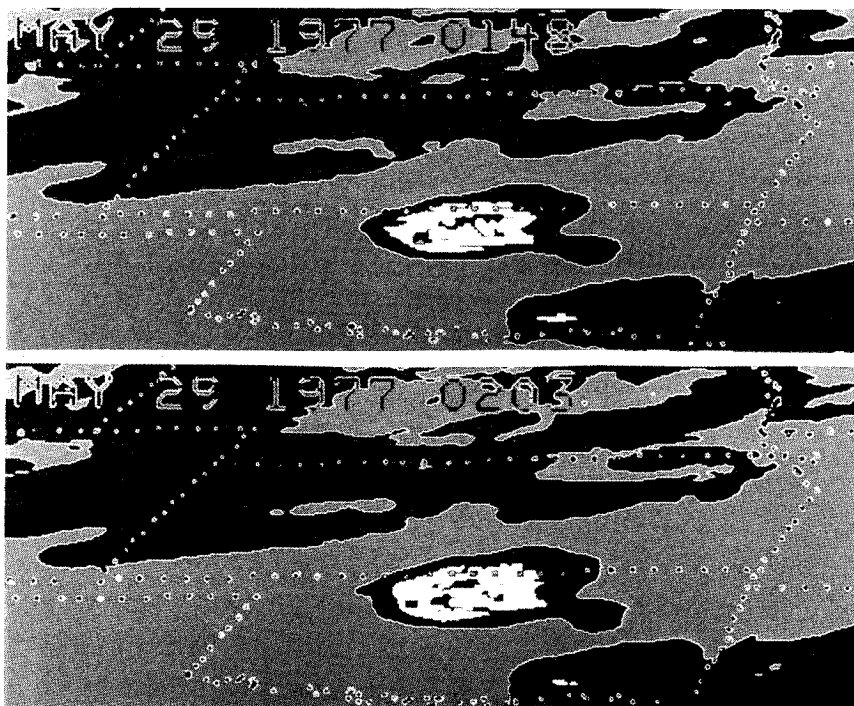


Fig. 9 Pseudocolor representation of the cloud top temperatures in Oklahoma and surrounding states from GOES infrared image at 0148 and 0203 GMT, May 29, 1977. The cloud system A reached a temperature $\leq -73.2^{\circ}\text{C}$ at 0148 GMT and showed collapse of height at 0203 GMT.



above the tropopause for cloud A was 605 pixels, while for cloud B it was 255 pixels. The total force required to support the large, tall cold dome of cloud A above the tropopause is a few times greater than that of cloud B. This is one of the major satellite-observable differences between cloud A, which produced a funnel cloud after the collapse of the overshooting turret, and cloud B, which dissipated without causing a funnel cloud.

Figure 12 shows the histories of the cloud top temperatures for clouds A and B. Cloud A first appeared on the visible images at 2333 GMT. Prior to that time the cloud top temperature, based on the infrared images in Fig. 12, showed a series of precursor oscillations of the boundary-layer moisture field before the upward air mass overcame the temperature inversion. The precursor oscillations will be discussed in the

next section. Although not included in the figure, a similar feature was also observed for cloud B. The figure shows that it took about 30 min for both clouds to penetrate above the tropopause after the clouds appeared on the visible images. Subsequently, the temperature of cloud A declined continuously to the lowest temperature, which occurred about 20 min before touchdown of the tornado. The temperature of cloud B maintained an almost constant value (the difference between the cloud top temperature and the tropopause temperature was within 3°C) and persisted for more than 3.5 h until the cloud dissipated.

Meteorological Background

Meteorological data show that there was no front in this area of Oklahoma during the time period of the satellite

observations. Gravity wave trains were detected in these time periods by the Doppler sounder array located in Huntsville, Ala.² Results of ray tracing show that a series of gravity waves was excited from the area of cloud A.² The association between gravity waves and severe convective storms has been shown extensively in the laboratories and in the field during

the past decade.⁹⁻¹² Recently, gravity waves associated with tornado activity¹³⁻¹⁸ and hurricanes¹⁹ have been observed. The observation of gravity waves initiated from cloud A indicates the existence of strong convection inside the cloud.^{2,9,10} If any short period waves (those having periods of 5 min) were excited by cloud B, they were too weak to be detected in the Huntsville area which is 400 km away from the wave source; however, the wave trains with periods of 15 min excited by cloud A were detected.² This is due to the fact that the damping rate of a wave is inversely proportional to the wave period, and only the waves with longer wave periods can propagate the longer distance without dissipation.²⁰

The stability of an air mass can be determined from rawinsonde observations. From the synoptic situation, both locations A and B should have been in the same air mass. On the 2300 GMT, May 28, 1977, Oklahoma City rawinsonde, the temperature lapse rate was dry adiabatic below 2.1 km (790 mb). The relative humidity was around 70% in this lower layer of the atmosphere. There were temperature inversions between 2.1 and 2.5 km and also between 4.4 and 4.5 km. The air mass was fairly unstable between 6.0 and 7.2 km, because the lapse rate was nearly dry adiabatic. Once this unstable air mass gained enough energy to penetrate the temperature inversions at 2.1 and 4.4 km, the updraft motion continued until the clouds reached the altitude of the tropopause. The precursor oscillations shown in Fig. 12 occurred at an altitude of about 4.5 km before the updraft air mass completely overcame the temperature inversion. Once the moist air mass penetrated above the temperature inversion at 2318 GMT for cloud A and 2131 GMT for cloud B, cloud A became large enough to be seen on the visible image at 2333 GMT and cloud B at 2201 GMT. The size of the cloud formed is partially dependent upon the amount of moisture available to provide the energy source for initiating the updraft motion.

The synoptic situation was such that warm moist air from the Gulf of Mexico had been moving into the area for several days prior to May 28, 1977. This led to an unstable layer below 2.1 km and a surface air temperature of 29°C. Although the entire area had been subjected to the same synoptic situation, low-level precursor oscillations followed by a short period of very rapid growth were observed at cloud system B approximately 1 h prior to their occurrence at cloud system A. The information available was not sufficient to establish either why the precursor oscillations and subsequent rapid growths occurred at only these two isolated locations rather than over the area as a whole or why there was approximately 1 h difference in the times of occurrence.

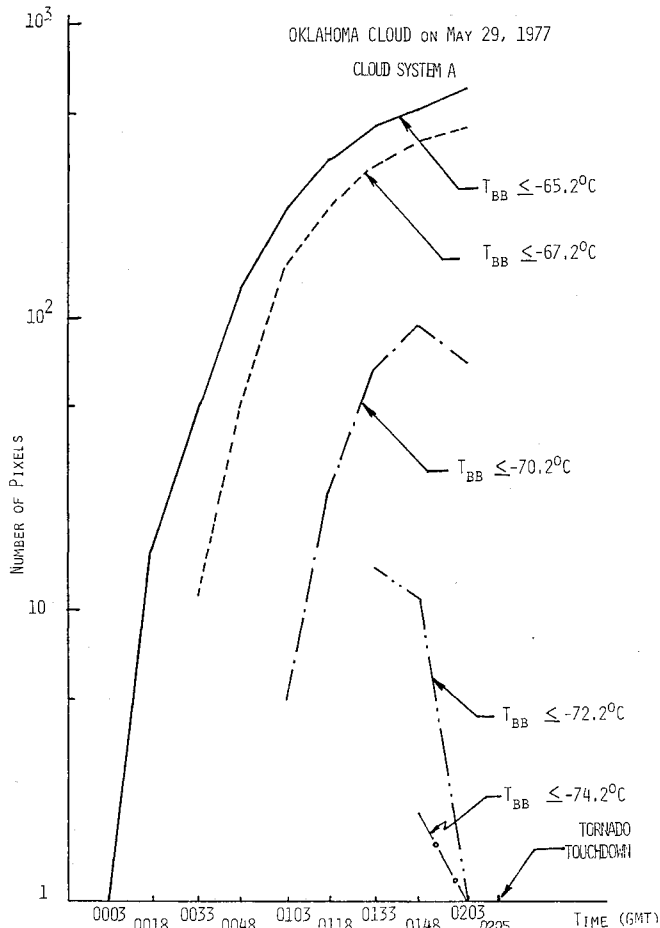


Fig. 10 Histogram of cloud system A after the penetration of tropopause.

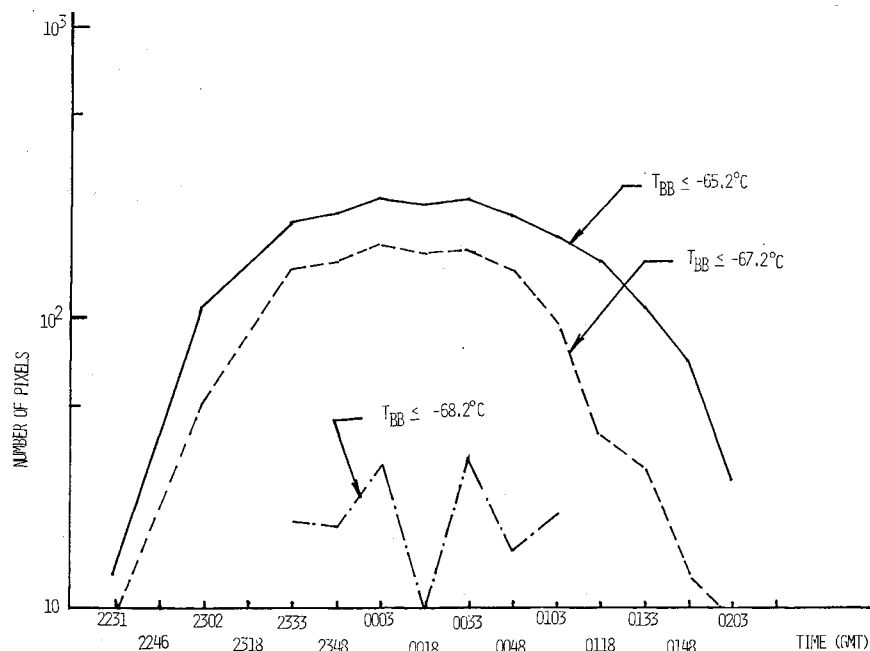
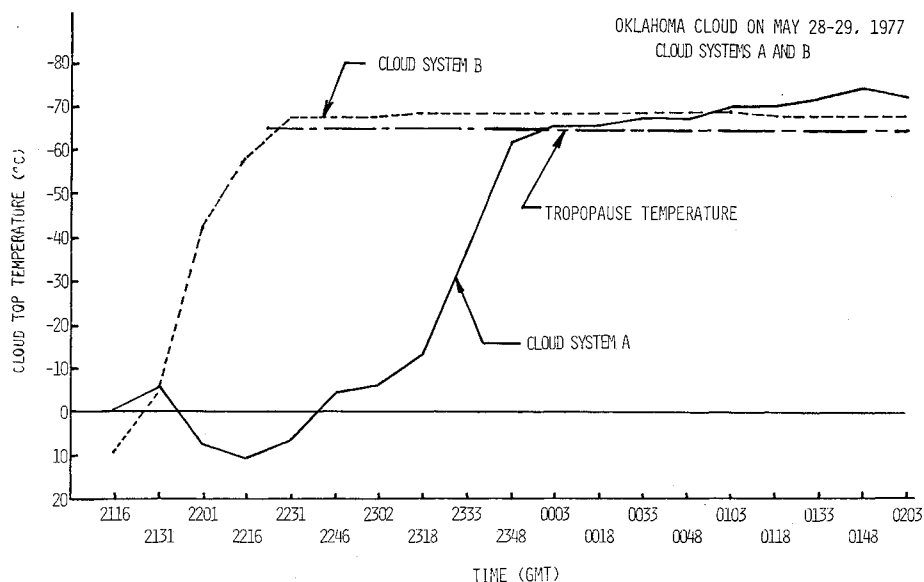


Fig. 11 Histogram of cloud system B after the penetration of tropopause.

Fig. 12 Histories of the cloud top temperatures for cloud systems A and B.



Discussions and Conclusions

Special rapid-scan satellite visible and infrared observations have enabled observation of two isolated clouds, one associated with a tornadic storm and one associated with a thunderstorm only, in the Oklahoma area. The satellite data have permitted study of the life cycle of the clouds from the initiation of condensation, through the formation of the clouds, the development of towering cumulus, the penetration of the tropopause, the collapsing of an overshooting turret, and the dissipation of the cloud. During the inception and developing stages of the clouds before they penetrated the tropopause, there are very few apparent differences between the cloud which spawned a tornado and that which ended as a thunderstorm. After penetration of the tropopause, the differences between the two cloud systems are more readily discernible using satellite observations. The basic characteristics of the cloud associated with the Ringwood tornado were 1) a large volume of cold cloud above the tropopause, 2) a higher growth rate for clouds above the tropopause (12.2×10^{-2} pixels $\cdot s^{-1}$ for the present case), 3) a cloud top temperature much lower than the tropopause, and 4) a rapid collapsing of the cloud top immediately prior to the touchdown of the funnel cloud. Characteristics of the cloud which terminated in a thunderstorm based on the present study were 1) a small volume of cold cloud above the tropopause, 2) a low growth rate for clouds above the tropopause (5.3×10^{-2} pixels $\cdot s^{-1}$ or lower for the present case), 3) a cloud top temperature not much lower than the tropopause temperature, and 4) a gradually dissipating cloud above the tropopause.

Since the temperature of the overshooting turret is much lower than that of the surrounding air, the density of the turret is much higher than the surrounding air density, and the overshooting turret can exist only as long as it is dynamically supported by intense vertical convection. The relation between the time rate of change of vertical momentum and energy released by moisture condensation can be shown as

$$\frac{d}{dt}(M_a V_z) = F_z = -\frac{dQ}{dz}$$

where M_a is the mass of the moist air, V_z the vertical velocity of the moist air mass, F_z the force in the vertical direction, and Q the total energy released from moisture condensation.

It is clear that, in order to support a tall, large and heavy overshooting turret above the tropopause, a large gradient of thermal energy is necessary. To overcome the temperature

inversions, in the present case at altitudes of 2.1 and 4.4 km, an updraft motion also had to be initiated which was assisted by a large gradient of thermal energy.

Severe convective storms are a mesoscale phenomena with a short life cycle of a few hours duration; therefore, rapid scans are necessary to insure obtaining effective observations of the future storm development. If the observations are more than 15 min apart, the collapsing of the cloud top just prior to the formation of the funnel cloud cannot be observed because the collapse of the cloud top normally occurs about 15-30 min before the touchdown of the tornado based on the case studies of March 24, 1976, April 11, 1976, and May 29, 1977. Neither the current ground- or satellite-based observations provide the temporal and spatial data coverage required to establish the detailed life cycles of clouds in mesoscale systems. Imaging systems with rapid-scan capabilities (less than 15 min intervals) and sounders with spatial resolutions on the order of 25-50 km would be required to insure adequate data coverage for these types of severe weather occurrences.

Areas of localized moisture convergence cannot be determined from the current rawinsonde observation network. In the present case, for example, while the air mass in general was unstable, there was no way to foresee that strong local moisture convergence areas would develop in north central and south central Oklahoma based on the rawinsonde observation from Oklahoma City. It remains to be seen if the proposed satellite sounder systems will provide the data to distinguish such localized areas.

Nevertheless, the present data illustrate the capability of infrared and visible images (from geosynchronous satellite) to describe the life cycles of tornadic clouds, such as 2116 GMT, May 28, to 0203 GMT, May 29, 1977, for cloud A shown in Fig. 12. There is evidence of differences between the clouds associated with tornadoes and those that are not after the clouds have penetrated above the tropopause. Earlier detection of severe storms might be possible if localized areas of moisture convergence and instability could be identified.

Acknowledgments

R. J. Hung appreciates the support of the present study from the National Aeronautics and Space Administration through Contract NAS8-33726.

References

- Purdum, J.F.W., "Some Uses of High Resolution GOES Imagery in the Mesoscale Forecasting of Convection and Its Behavior," *Monthly Weather Review*, Vol. 104, Dec. 1976, pp. 1474-1483.

- ²Hung, R. J., Phan, T., Lin, D. C., Smith, R. E., and Jayroe, R. R., "Gravity Waves and GOES IR Data Study of an Isolated Tornadoic Storm on 29 May 1977," *Monthly Weather Review*, Vol. 108, April 1980, pp. 456-464.
- ³Adler, R. F. and Fenn, D. D., "Thunderstorm Intensity as Determined from Satellite Data," *Journal of Applied Meteorology*, Vol. 18, April 1979, pp. 502-517.
- ⁴Adler, R. F. and Fenn, D. D., "Satellite-Observed Cloud Top Height Changes in Tornadoic Thunderstorms," *Journal of Applied Meteorology*, Vol. 20, Nov. 1981, pp. 1369-1375.
- ⁵Gentry, R. C., Rogers, E., Steranka, J., and Shenk, W. E., "Predicting Tropical Cyclone Intensity Using Satellite-Measured Equivalent Blackbody Temperature of Cloud Tops," *Monthly Weather Review*, Vol. 108, April 1980, pp. 445-455.
- ⁶Sikdar, D. N., Suomi, V. E., and Anderson, C. E., "Convective Transport of Mass and Energy in Severe Storms over the United States—An Estimate from a Geostationary Altitude," *Tellus*, Vol. 22, 1970, pp. 521-532.
- ⁷Fujita, T. T. and Caracena, F., "An Analysis of Three Weather-Related Aircraft Accidents," *Bulletin of the American Meteorological Society*, Vol. 58, Nov. 1977, pp. 1164-1181.
- ⁸Fujita, T. T. and Byers, H. R., "Spearhead Echo and Downburst in the Crash of an Airliner," *Monthly Weather Review*, Vol. 105, Feb. 1977, pp. 129-146.
- ⁹Willis, G. E. and Deardorff, J. W., "A Laboratory Model of the Unstable Planetary Boundary Layer," *Journal of the Atmospheric Sciences*, Vol. 31, July 1974, pp. 1292-1307.
- ¹⁰Curry, M. J. and Murty, R. C., "Thunderstorm-Generated Gravity Waves," *Journal of the Atmospheric Sciences*, Vol. 31, July 1974, pp. 1402-1408.
- ¹¹Gossard, E. and Sweezy, W. B., "Dispersion and Spectra of Gravity Waves in the Atmosphere," *Journal of the Atmospheric Sciences*, Vol. 31, Aug. 1974, pp. 1540-1548.
- ¹²Uccellini, L. W., "A Case Study of Apparent Gravity Waves Initiation of Severe Convective Storms," *Monthly Weather Review*, Vol. 103, June 1975, pp. 497-513.
- ¹³Hung, R. J., Phan, T., and Smith, R. E., "Observation of Gravity Waves during the Extreme Tornado Outbreak of April 3, 1974," *Journal of Atmospheric and Terrestrial Physics*, Vol. 40, July 1978, pp. 831-843.
- ¹⁴Hung, R. J., Phan, T., and Smith, R. E., "Ionospheric Doppler Sounder for Detection and Prediction of Severe Storms," *AIAA Journal*, Vol. 16, July 1978, pp. 763-766.
- ¹⁵Hung, R. J., Phan, T., and Smith, R. E., "Case Studies of Gravity Waves Associated with Isolated Tornadoic Storms on January 13, 1976," *Journal of Applied Meteorology*, Vol. 18, April 1979, pp. 460-466.
- ¹⁶Hung, R. J., Phan, T., and Smith, R. E., "Coupling of Ionosphere and Troposphere during the Occurrence of Isolated Tornadoes on November 20, 1973," *Journal of Geophysical Research*, Vol. 84, April 1979, pp. 1261-1268.
- ¹⁷Hung, R. J. and Smith, R. E., "Ray Tracing of Gravity Waves as a Possible Warning System for Tornadoic Storms and Hurricanes," *Journal of Applied Meteorology*, Vol. 17, Jan. 1978, pp. 3-11.
- ¹⁸Hung, R. J. and Smith, R. E., "Dynamics of Severe Storms through the Study of Thermospheric-Tropospheric Coupling," *Journal of Geomagnetism and Geoelectricity*, Vol. 31, May 1979, pp. 183-194.
- ¹⁹Hung, R. J. and Kuo, J. P., "Ionospheric Observation of Gravity Waves Associated with Hurricane Eloise," *Journal of Geophysics*, Vol. 45, Jan. 1978, pp. 67-80.
- ²⁰Hung, R. J., Wu, S. T., and Smith, R. E., "Propagation of Acoustic Modes in the Transitional Ionosphere," *Journal of Geophysical Research*, Vol. 80, Nov. 1975, pp. 4325-4330.